

Role of the CdS/ZnS core/shell quantum dots in the thin film lead-free perovskite solar cells

M. P. Aleksandrova^{1*}, G. D. Kolev¹, R. Tomov¹, A. K. Singh², K. C. Mohite³, G.H. Dobrikov¹

¹Technical University of Sofia, Dept. of Microelectronics, 8 Kliment Ohridski Blvd, 1000 Sofia, Bulgaria

²Govt. V.Y.T.P.G. Autonomous College, Dept. of Chemistry, Near Raipur Naka, G.E. Road, Durg, India.

³University of Pune, Ganeshkhind Rd, Ganeshkhind, Pune, Maharashtra 411007, India

The performance of the thin film solar cells has been enhanced in recent years by development of new materials broadening the spectral response of the cell and suppressing the long wavelength absorption close to the near infrared range. Absorber layers are developed to improve the collection of photo-carriers when perovskites are used as photoelectric converting films. This is due to the easy tuning of the energy levels alignment at the films interface. For the new types of lead-free perovskites, the interaction between sulphide based absorber and the perovskite is not yet investigated. First, the deposition and processing conditions for the perovskite coatings were optimized in terms of crystallization degree and uniform surface. The perovskite films crystal morphology and the crystal growth kinetics were found to be similar like the films' morphology consisting of organic molecules having non-perovskite structure. Optimized perovskite films, containing this absorber with different thickness were applied in combination with lead-free perovskite films. Homogeneous core/shell type CdS/ZnS films with high density were produced. Simple cell construction is proposed, containing ITO/ZnO:Ga₂O₃ front panel electrode, lead-free CH₃NH₃I_{3-x}Cl_x based perovskite and gold back contact. The cells were tested at open circuit conditions at different illumination intensity and different wavelength of the illuminating source. At optimal conditions the fabricated solar cells showed which 1.9% higher conversion efficiency, to the reference cell without absorber. The results demonstrated the applicability of the lead-free perovskite material and the effect of sulphide layers on the solar cell electrical parameters improvement. This is a basic step to further optimization of this technology.

Keywords: sulphide absorber layer, quantum dots, core/shell technology, perovskite photoconductor, lead-free solar cell

INTRODUCTION

In recent years, the Perovskite solar cells have been developed dramatically, due to their low-cost and simple fabrication, especially the hybrid ones, containing organic and inorganic constituents, such as CH₃NH₃PbI₃ for example [1]. For ten years the materials science technology has allowed 6 times increase in the power conversion efficiency. In 2018 has been reported about 23.3% produced from devices with size of 1 cm² [2].

General formula for perovskite is ABX₃, in which A is monovalent cation, B is divalent cation (i.e., Pb²⁺/Sn²⁺/Pd²⁺ etc.) and X is halide ion, it is the base of solar cell. ABX₃ halide perovskite is a photovoltaic material and has shown higher efficiency in solar cell technology compared to cadmium-tellurium material. By deep literature study we observed that electronic configuration of lead (Pb²⁺) is mainly responsible for photovoltaic behavior of solar cell. Lead based perovskite solar cell still has limited use because many countries have strict regulation for use of heavy metal ions, so research now focused on making lead free perovskite solar cells [3-5].

Nowadays, the hybrid perovskite solar cells with their electrical and optical parameters are competitive to the well-established thin film technology for photoelectric convertors based on cadmium telluride CdTe and copper indium gallium selenide (CIGS). A lot of researches have been conducted to achieve this goal, related to thin film quality. It seems that the favourable behaviour of these modules is due to the broad absorption of the solar spectrum, because of the presence of lead as a core chemical element in the perovskite material. The new trends worldwide for implementation of environmental friendly materials and technologies, excluding the lead-containing substances have made further development of these solar cells senseless. The focus has been shifted on the synthesis of new, eco-friendly perovskites, in which the lead is replaced by Br, Sb, or I [6].

There are various methods were reported for synthesis of thin film of perovskite solar cell, e.g., sequential deposition, one step, vapour assisted solution process and vapour deposition method [7]. However, spin coating method is one of the best, cost effective and efficient methods [8]. An alternative approach for producing planar perovskite thin films based on combination of RF-sputtering with the solution process route.

Rahul et al., have fabricated a new class of

* To whom all correspondence should be sent:
m_aleksandrova@tu-sofia.bg

material ($\text{CH}_3\text{NH}_3\text{SnCl}_3$) to prepare lead free perovskite solar cell by direct deposition method. It is environment friendly and cost effective too [9]. Balakrishna et al. have reported effect of iodide treatment on stability of perovskite solar cell [10]. Li et al. have reported a mini review on lead free and less lead containing perovskite solar cell and possible solution for its stability and photoelectric performance [11]. Nakajima et al. have used computation software using Density functional theory, to study various organic-inorganic materials to find out perfect combination of environment friendly perovskite solar cell and they proposed 51 low toxic double and single halide combinations [12]. Baenstein et al. have replaced lead in halide perovskite and replace it by combination of mono and trivalent cation as a bulk single crystal and a thin layer [13].

Because their natural bandgap is narrower in comparison with those of the hybrid solar cells (mostly in the range 450-550 nm), the conversion efficiency has dropped to 2 %. Some of the important results in the field have been published by Jiang et al. in 2018, who has reported greater efficiency when Cl is incorporated as a light absorber in a complex perovskite (CH_3NH_3) $3\text{Sb}_2\text{Cl}_x\text{I}_{9-x}$ [14]. At present, still many challenges must be overcome before the commercialization of the perovskite solar cells, which hinder their broad application. Appropriate materials and designs still have to be proposed to solve the problem with the low power conversion efficiency, toxicity of some solvents and great sensitivity to radiation out of the visible range make their long-term stability under question.

Adding multilayer absorber film stack into the structure, like CdSe/ZnS, for example, is one of the current approaches of interest to improve the performance of cells due to extension of the absorption ability in a broader wavelength range. Some authors report for insertion of similar films with this function, subjected to annealing for interdiffusion and complex compound achieving such as $\text{CdSe}_x\text{Te}_{1-x}$, with only partial control over the exact composition [15]. Recently, the core/shell technology has offered a great advantage of no leakage of excited electrons, better energy level alignment with the surrounding coatings, and higher quantum yield [16]. These materials have higher efficiency to absorb solar energy and to convert it into electrical energy.

In this study, we propose to enhance the light conversion ability of a solar cell containing lead-free perovskite material by inserting sulphide based

absorbing films of core-shell type. To the best of our knowledge such study has not been conducted and reported in the literature so far. For this purpose, absorber layers with different thicknesses were introduced and the basic characteristics of the cell were measured. The results show that using additional absorption layers can gain the long wavelength absorption, thus increasing the cell performance, while the short wavelength response is not changed. The effect of the ambient environment on the perovskite films was also studied and suitable pre- and post-deposition processing was proposed in order to reduce the degree of random crystallization effect. Secondary benefits from the study are the conclusions that can be made for the wetting ability of the $\text{ZnO}:\text{Ga}_2\text{O}_3$ (GZO) transporting layer from the perovskite ink as a novel concept for front panel filter of the sun heating component decreasing the solar cells' efficiency.

EXPERIMENTAL SECTION

Perovskite photoconductive film was spin coated on glass/ITO (180 nm)/ $\text{ZnO}:\text{Ga}_2\text{O}_3$ (GZO, 100 nm) substrates. The glass substrate was cleaned in standard detergent solution including ammonia, hydrogen peroxide and distilled water. Indium tin oxide was RF sputtered at sputtering pressure of 10^{-3} Torr and sputtering voltage of 700 V, followed by RF sputtering of $\text{ZnO}:\text{Ga}_2\text{O}_3$ at the same sputtering pressure and sputtering voltage of 850 V. Recently, we found that GZO can serve as efficient front panel transporting layer, supporting the function of the transparent ITO conductor, but at the same time exhibiting optical rejection ability in the near infrared spectrum. It could successfully replace the conventionally used in the perovskites solar cells TiO_2 film, serving only as a transporting layer [17]. Methyl ammonium iodide chloride based perovskite ink was spin coated at 1000 rpm per 30 sec and consequently dried for 10 min at 130 °C. Preliminary simulation showed that the optimum layer in terms of suppressing parasitic electrical losses in the cell is 300 nm [18]. Open-source software combining the features of Silvaco and PC1Dmod was used. The basic equations rely on the Boltzmann equations with the assumptions that the two carriers flow independently without scattering, both types charge carriers (positive and negative charges) remain in thermal equilibrium with the surrounding matter (no matter crystalline or non-crystalline), and the energy levels form rigid bands, i.e. not affected by the excitation. The software considers direct-gap and indirect-gap

transitions. The front and rear surface reflections are calculated based on the refractive indices and thicknesses of thin films and the substrate following the Fresnel's equations. The absorption from the substrate obeys the Lambert-Beer law. Considering the hybrid nature of the cell (organic-inorganic) for this case the description of charge transport at hetero-interfaces follows the model of Miller-Abrahams and the recombination processes – the model of Kerr and Cuevas. Top gold electrode with thickness of 120 nm was deposited by DC sputtering. Core/shell CdS/ZnS quantum dots (QDs) were spin-coated from carboxylic acid dispersion at 500 rpm with additional drying at 70°C for 10 min. These films were used as absorbers in the cell structure and they were placed in front of the perovskite films. Variety of CdS/ZnS QDs monolayers were produced by different number of consequent dispersion casting to study the effect of the absorbing layer thickness on the solar cell characteristics. One casting provides ~60 nm thickness of the coating (1 layer = ~60 nm; 2 layers = ~120 nm). Schematic drawing of the device structure is shown in Fig.1.

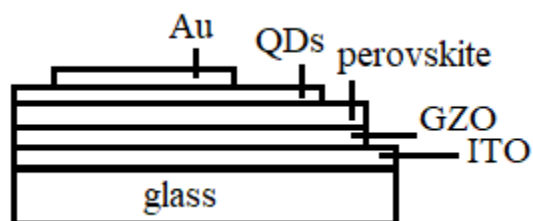


Fig.1. The structure of the proposed lead-free perovskite solar cell

The area of the fabricated samples was 3 cm². For the open circuit mode a light source with white spectrum and maximum power of 100 μW/cm² was set to avoid a crowd effect in the films, serving as shallow reservoirs for the excited charge carriers. For the closed circuit mode (with load) colour filters were used to pass selectively one of the three basic wavelengths – red, green and blue – for spectral sensitivity study. The thickness of the films was measured by surface profilometer Alpha-step Tencor 100 VEECO. The roughness of the thin film surface is observed by atomic force microscope (AFM) Oxford Instruments MFP-3D. The optical absorption and transmission of the films was measured by using spectrophotometer UV VIS NU-T6PC Zhengzhou Nanbei Instrument. Current-voltage (IV) characteristics of the perovskite thin film solar cells were measured by Agilent 34410A voltmeter and picoamperemeter Keithley 6482 after calibration with a GaAs reference cell. The

efficiency of the solar cells was measured by the Thorlabs PDA200C Benchtop Photodiode Amplifier.

RESULTS AND DISCUSSION

The initial experiments related to the spin-coating of the perovskite ink on the transparent electrode showed that the ink distribution is not uniform due to the poor wetting ability of the substrate (Fig.2). Additionally, random crystallization centres were revealed with diameter almost 156 μm worsening further the quality of the coating after exposure the samples to direct contact with the ambient and hard baked at 130 °C.



Fig.2. Microscopic image of the perovskite coating at the initial deposition of perovskite ink on the glass/ITO/ZnO:Ga₂O₃ substrates

Interesting effect that needs further investigation of its formation mechanism is the crystallization degree dependence on the perovskite coating thickness. It was observed that the films with a thickness in the range 200-250 nm exhibited stronger tendency to form network of local crystallizing centres as compared to the thicker films in the range 500-550 nm (Fig.3) at one and the same ambient conditions. Study of such dependence was recently reported about ultrathin organic molecules containing films with varying thickness in the range of 34-220 nm [19]. The kinetics of the crystallization process showed similar trends, which was ascribed to the non-linear dependence of the crystallization rate with the film thickness, according to the Lauritzen-Hofman growth. It could be assumed that the same model could be fitted in the case of perovskite films.

It was applied pre-deposition treatment with UV light (365 nm), so that the ultraviolet exposure can break the bonds from the surface states of the coating making them dangling. It was previously demonstrated that the approach increased the free energy on the surface and the wetting susceptibility from inks [20]. Additionally, the film growth was conducted in ambient air-free environment and

baked at lower temperature of 100 °C to avoid fast solvent evaporation (Fig.4). Notable improvement of the surface morphology was observed with very few crystallization centres formed.

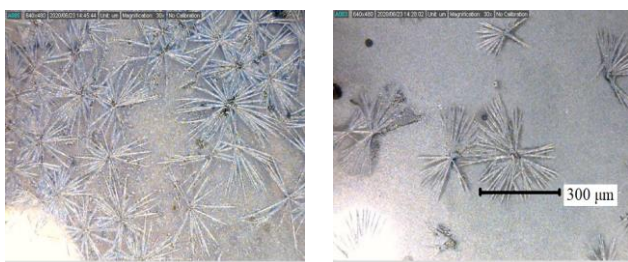


Fig.3. Microscopic image of the perovskite coatings with different thicknesses - 230 nm (left) and 540 nm (right)



Fig.4. Microscopic image of the perovskite coating at the optimized deposition of perovskite ink on the glass/ITO/ZnO:Ga₂O₃ substrate

The conditions for substrate pre-treatment, spin-coating and drying conditions for the perovskite films deposition and the film crystallization qualitative evaluation were summarized in Tab.1, considering the ultraviolet exposure pre-treatment and the type of ambient (inert or not).

Table 1. Summarized growth conditions for the perovskite films

UV treat.	Spinning	Drying	Crystallization
no	1000 rpm	130°C amb.	Strong
no	2500 rpm	130°C amb.	Much stronger
yes	1000 rpm	130°C inert	Average to low
no	1000 rpm	100°C inert	Average to low
yes	1000 rpm	100°C inert	Low

Fig.5 shows the visible absorption spectra for: perovskite only layer (reference cell); CdS/ZnS core/shell/perovskite layer with 1 layer; CdS/ZnS core/shell/perovskite layer with 2 layers. It was noted that the increase of the core/shell thickness

resulted in a shift of the overall absorption spectra to the higher wavelength. Moreover, the absorption of the cells with double core/shell layer is approximately 20 % greater in the long wavelength range than the reference cell. Overall, the light absorption of these absorbing layers is greater, as compared to CdSe, for example. The total absorption shift was approximately 22 nm. Therefore, the thickness of this layer can control the absorption spectrum in terms of broadening, or shortening, causing a peak position to vary.

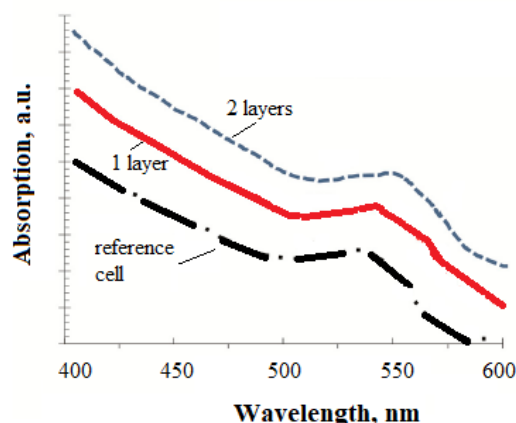


Fig.5. Absorbance spectra of the perovskite films without absorber layer (reference cell) and with different number of CdS/ZnS core/shell layers

The AFM 2-dimensional images (top view) of the perovskite films without absorber layer (reference cell) and with different number of CdS/ZnS core/shell layers are shown in Fig.6, from which the particle distribution and film homogeneity can be visualized.

The surface of the films in all studied cases was found dense and homogenous with roughness of 32 nm, 28 nm and 20 nm, respectively for the perovskite films without absorber layer (Fig.6a), for the single layered CdS/ZnS core/shell (Fig.6b) and for the double layered CdS/ZnS (Fig.6c). Compared with perovskite films only, the surface roughness decreases with the core/shell thickness increases.

The J-V curves corresponding to different CdS/ZnS core/shell films thickness are shown in Fig.7 at white light with radiometric intensity of 0.05 mW/cm² without load. Single layer core-shell seems not sufficient to support for longer time the absorption phenomena of the photons. Although at the beginning such conditions exist it is quickly degraded due to the small concentration of light absorbing QDs in one layer. In addition, although the surface roughness of the system perovskite/CdS/ZnS is lower as compared to the

reference cell, it is still not sufficient to guarantee uniform contact and small interface resistance with the electrodes. At higher current densities of ~ 4 mA/cm² this drawback didn't manifest, but as the current density got smaller as the sensitivity to this contact resistance effect got stronger, which imposed application of two-layered structure of the absorber. Similar effect has been observed in [21] for CdSe_xTe_{1-x}/CdTe cells, where such behaviour has been also ascribed to the contact resistance, however caused by the multiple thin film interfaces.

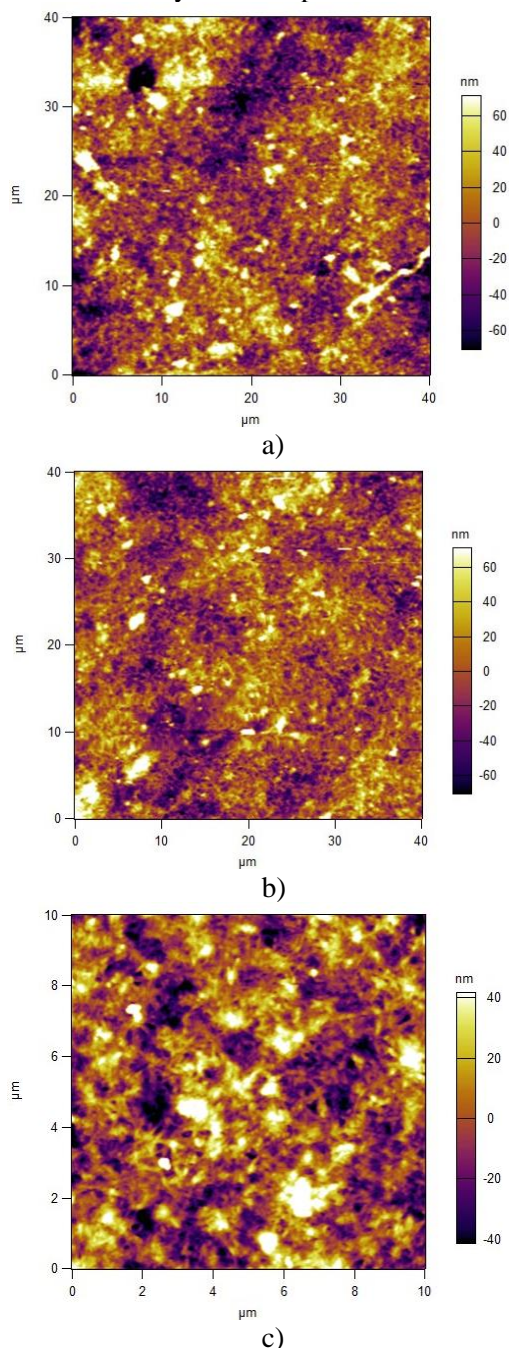


Fig.6. AFM 2D surface morphology of a) perovskite film without absorber layer (reference cell) b) single CdS/ZnS core/shell layer; c) double CdS/ZnS core/shell layer

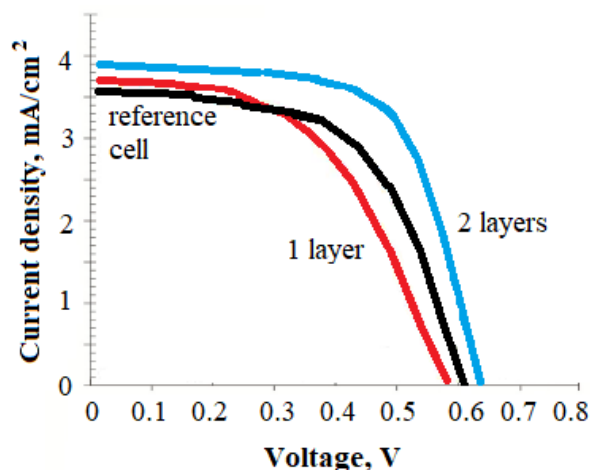


Fig.7. Current-voltage characteristics comparing the light performance of the cells with different core/shell layer thickness against a reference device

The effective band gap of the absorbing layer was calculated, following methodology described elsewhere [22], based on the cut-off edge of the quantum efficiency curve at the long wavelength visible/NIR boundary. According to it, the increase of the thickness of the core/shell layer as compared to the reference, absorber-free cell, resulted in a shift of the cut-off edge toward the longer wavelength without affecting the short wavelength range. It varied from 1.45 eV at zero thickness to 1.42 eV at the optimal thickness.

The device exhibited the best performance at a thickness of the core/shell layer of ~ 120 nm. The highest efficiency of 16 % was reached with back gold electrode. The maximum current density reached almost 4 mA/cm² at 120 nm thickness of the CdS/ZnS (for comparison, for the reference cell, a current about 3.5 mA/cm² was measured). Open circuit voltage is also increasing with the CdS/ZnS thickness (from 0.57V to 0.63V), although its change of 60 mV is more insignificant.

The change of the solar cell efficiency at thickness of the core/shell layer of 120 nm, as compared to the reference cell is shown in Fig.8.

In the paper [18] it was demonstrated the double function ability of the absorbing layer - it can function not only as an absorber, but also as a back buffer for balancing the charges path for which the maximum diffusion length was achieved at a thickness of 300 nm (considering the difference in the charge carriers mobility existing in the cell). When it is not used as a buffer (i.e. transporting layer), its thickness should be significantly reduced to avoid contribution of potential defects for the light scattering and optical losses. Thus, some

approximate ratios known from the literature with similarity to the non-perovskite cells were used as a starting point to determine the thickness of the absorber [23]. Higher than the maximal used in this study thickness destroyed the balance in the light penetration against the diffusion coefficient of the charge carriers injected and increased the reflectivity, leading to negative effect of electrical energy drops, because of the worsen collection efficiency (not shown).

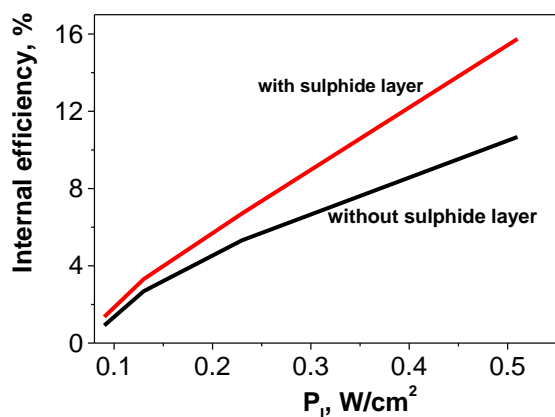


Fig. 8. Comparison between the efficiency of the solar cell without and with buffer absorbing layer at white light [18]

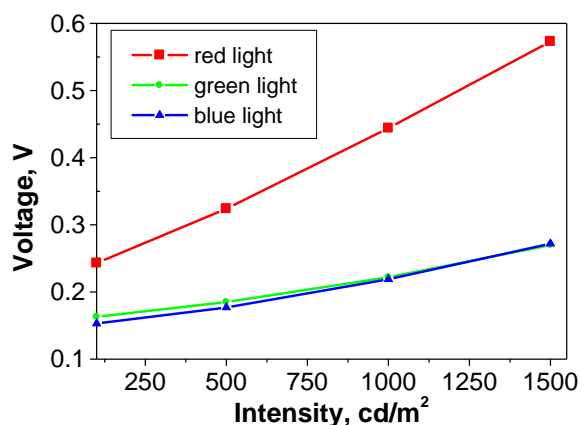


Fig. 9. Voltage vs. intensity at different light colours for the optimal solar cell with attached electrical load

Study of the produced voltage's spectral sensitivity of the sell with buffer layer at photometric intensity in the range of 100-1500 cd/m^2 , with light-emitting diode (LED) attached as a load, showed the greatest values produced at the red light (Fig.9). It was measured maximum 573 mV at 1500 cd/m^2 and minimum 243 mV at 100 cd/m^2 . In contrast, poor sensitivity was

demonstrated for green and blue light, with almost twice lower and similar maximum voltages for both wavelengths, varying between 153 mV and 272 mV in the whole range of intensities.

Comparison with the widespread CdS/CdTe based cells showed that the absorption of the present structure near the long-wavelength region is notably increased, indicating that the light absorption range of the absorber in the studied devices is broader. Therefore, the quantum efficiency in this region is expected to be significantly enhanced, which is shown with the corresponding electrical power spectral sensitivity, shown in Fig.10. This is in line with previous report [24] and additionally confirms the results from the absorbance spectra.

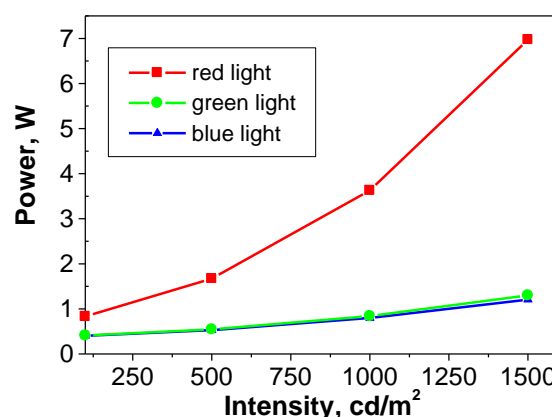


Fig. 10. Electrical power vs. intensity at different light colours for the optimal solar cell with attached electrical load

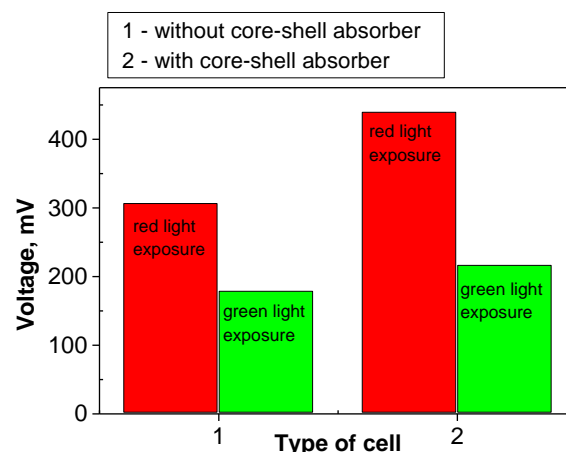


Fig. 11. Comparison of the voltages produced from cells with and without core-shell absorber at different wavelengths of the exposure light

The performance of the cell and the influence of the absorber layer can be also estimated by direct comparison between the photogenerated voltage in

open circuit mode for perovskite ink and for core-shell/ink structures at 1000 cd/m² (Fig.11).

CONCLUSIONS

In summary, solar cell with perovskite lead-free coatings were prepared and investigated. The perovskite films crystal morphology was found to be similar like the growth kinetics of organic containing molecules with non-perovskite structure. The evolution of the crystallization centres formation and films morphology was followed according to the ambient and processing condition. A double layered core/shell CdS/ZnS material was applied by casting to change the film morphology in the solar cell. With the increase of the layer thickness, the morphology of the film changed noticeable. Improved optic conditions in the long wavelength range can be noted, which affects in a decrease of the bandgap and improved current and voltage generated conditions. As a general conclusion, it can be said that the absorbing core/shell layer with optimized thickness is a crucial part to improve the efficiency of lead-free perovskite solar cells.

As the power is produced on a simple resistive load only as a demonstrator for successful energy transfer to a load, our future work will be related to the power supplying a consumer like battery, backup supercapacitor and integrating circuit for smart photoelectric sensor, and then to determine the work point, fill factor and efficiency of the cell with respect to its size, constructive design and external connection.

ACKNOWLEDGEMENTS

This work has been supported by the joint project for bilateral cooperation in science and technology Bulgaria - India – KII06-India-6.

REFERENCES

[1] Chen Q. et al. *Nano Today*, **10**, 355-396 (2015).
 [2] M. Yang et al. *ACS Energy Lett.*, **3**, 322–328 (2018).
 [3] Noel N. K. et al. *Energy Environ. Sci.*, **7**, 3061–3068 (2014).
 [4] Hao F., Stoumpos C.C., Cao D.H., Chang R.P.H., Kanatzidis M.G. *Nat. Photon.*, **8**, 489–494 (2014).

[5] Zhao Z., et al. *Adv Sci (Weinh)*, **4**, 1700204 (2017).
 [6] Zhang Q. et. al. *Sci Technol Adv Mater*, **19**, 425–442, (2018).
 [7] Song T. B., Chen Q., Zhou H., Jiang C., Wang H. H., Yang Y., Liu Y., You J., Yang Y. *J. Mat. Chem.: A*, **3**, 9032-9050 (2015).
 [8] Rivera C. P., Cambero L. S., Torres M. S., Lima E., Ibarra D.S. *ACS Energy Lett.*, **3**, 2835–2840 (2018).
 [9] Rahul P. K., Singh R., Singh V., Singh B., Bhattacharya Z., Khan H. *Mat. Res. Bul.*, **97**, 572-577 (2018).
 [10] Balakrishna R. G., Kobosko S. M., Kamat P. V. *ACS Energy Lett.*, **3**, 2267–2272 (2018).
 [11] Li Q., Zhang P., Yao L., Deng L., Ren X., Li Y. *Int. J. Electrochem. Sci.*, **12**, 4915-4927 (2017).
 [12] Nakajima T., Sawada K., *J. Phys. Chem. Lett.*, **8**, 4826–4831 (2017).
 [13] Bakenstein Y., Dahl J. C., Huang J., Osowiecki W. T., Swabeck J. K., Chan E. M., Yang P., Alivisatos A. P. *Nano Lett.* **18**, 3502-3508 (2018).
 [14] Jiang F. et. al., *J. Am. Chem. Soc.*, **140**, 1019–1027 (2018).
 [15] Paudel N. R., Yanfa Y. Current enhancement of CdTe-based solar cells. *IEEE 42nd Photovoltaic Specialist Conference (PVSC)*, 14-19 June 2015, USA (2015).
 [16] Amira R. Abou Elhamd, Khaled A. Al-Sallal, Ahmed Hassan. *Energies*, **12**, 1058 (2019)..
 [17] Aleksandrova M., Ivanova T., Gesheva K., Strijkova V., Tsanev T., Singh J., Singh A. K. *Mat. Proc.*, **2**, 1-4 (2020).
 [18] Aleksandrova M. P., Kolev, G. D. Tomov, R., Singh, A. K., Mohite, K. C., Dobrikov, G.H., *Proc. of the 3rd Int. conf. "Alternative Energy Sources, Materials & Technologies (AESMT'20)"*, 8-9 June 2020.
 [19] Khairuddin, *J. Phys. Conf. Ser.*, **776**, 012055 (2016).
 [20] Aleksandrova M., Kurtev, N. Videkov V. Tzanova S., Schintke S. *Microelectron. Eng.* **145**, 112-116 (2015).
 [21] Li C., Li Ch, Wang Y., Ren S., Wang H., Wang W., Zhang J., Feng L. *Mat. Sci. Semicon. Proc.*, **121**, 105341 (2021).
 [22] Naba R. Paudel and Yanfa Yan. *Appl. Phys. Lett.* **105**, 183510 (2014).
 [23] Moon Md. M. A., Ali Md. H., Rahman Md. F., Hossain J., Ismail A. B. Md. *Phys. Stat. Sol.*, **217**, 1900921 (2020).
 [24] Swanson D. E., Sites J. R., Sampath W. S. *Sol. En. Mat. and Solar Cells.*, **159**, 389-394 (2017).